ELSEVIER

Polymer 42 (2001) 521–533

polymer

www.elsevier.nl/locate/polymer

A molecular simulation study on gas diffusion in a dense poly(ether–ether–ketone) membrane

E. Tocci[a,*], D. Hofmann[1,b], D. Paul[b], N. Russo[2,c], E. Drioli[a]

[a]*Institute on Membrane and Chemical Reactors—CNR c/o Department of Chem. Eng. and Mater., University of Calabria, I-87030 Arcavacata di Rende, Italy*
[b]*GKSS Research Center, Institute of Chemistry, Kantstr. 55, D-14513 Teltow, Germany*
[c]*Department of Chemistry, University of Calabria, I-87036 Arcavacata di Rende, Italy*

Received 31 May 1999; received in revised form 19 January 2000; accepted 28 January 2000

Abstract

Results of molecular dynamics (MD) simulations on transport and solubility of small molecules in amorphous cardo poly–ether–ether–ketone membranes are discussed. Atomistic simulation techniques have proven to be a useful tool for the understanding of structure–property relationships of materials. Although MD are still not an ideal tool for the quantitative prediction of gas permeation properties, this methodology can be used for a detailed description of the complex morphologies and transport mechanisms associated with rigid glassy structures.

The diffusion process results from jumps of penetrant molecules between adjacent holes in the polymer matrix. The free volume and the occurring jump mechanism are characterized and visualized with different methods. Constants of diffusion and solubility coefficients have been calculated by the Transition State Gusev–Suter Monte Carlo method revealing a considerable agreement between simulated and calculated data.

Keywords: Cardo poly(ether–ether–ketone); Molecular dynamics; Transport properties

1. Introduction

Computer simulation studies of permeation of small gas molecules through polymeric materials have undergone a remarkable development over the past few years. Detailed molecular dynamics simulations have become a widely used method for the investigation of the molecular structure of amorphous polymers and of the diffusion and solubility of small molecules through these materials. A number of Molecular Dynamics (MD) and Monte Carlo (MC) simulations of diffusion of small molecules in amorphous and semicrystalline polymers appeared [1,2] in the literature.

Most of these simulations deal with gas diffusion in the bulk of flexible chain polymers composed of rather simple monomers like PDMS and poly(isobutylene) [3–14], poly(ethylene) and poly(propylene) [15–17]. Few papers on MD simulations on stiff chain polymers are reported [18–20]. An MD simulation has been carried out by Chen et al. [21] on PEEK. The results indicate that in amorphous state ether–ether rings are more mobile than ether–ketone rings and in general that average mobility of large segments is reduced in comparison with simple phenylene rings.

There is an increasing interest of membrane researchers to explore the predictive power of the computational methods to calculate gas diffusion coefficients and solubilities with accuracy comparable with experiments. This interest is due to the increasing industrial role of polymeric membranes [22] in the separation treatment of gas streams.

Molecular modeling of glassy materials has been helpful in describing the complex morphology and the short time dynamics of the structures. Computer detailed atomistic modeling has however still some limitations due to the system size of simulated material that is still restricted to a few thousand atoms and the simulation time that is on the order of 10 ns with modern workstations.

Gas separation by amorphous polymers membranes can be described in a first approximation by continuum models with the solubility-diffusion type mechanism in which permeants dissolve in the membrane material and then diffuse through the membrane down a concentration

* Corresponding author. Fax: + 39-0984-402103.
E-mail addresses: hofmann@gkss.de (D. Hofmann); nrusso@unical.it (N. Russo).
[1] Fax: + 49-3328-46452.
[2] Fax: + 39-0984-492106.

0032-3861/01/$ - see front matter
PII: S0032-3861(00)00102-6

gradient with a final desorption of a permeate molecule at the downstream surface of the membrane [23,24].

A separation is achieved between different permeants because of differences in the amount of penetrant that dissolves in the membrane and the rate at which it diffuses through. The entire process of isothermal diffusion can be described by the two Fick's laws [25]. The permeability coefficient P, defined by the ratio between the flux J of the permeant species and the concentration gradient over the thickness d of membrane.

$$P = J\frac{d}{\Delta c} \tag{1}$$

is given by the product of the diffusion coefficient D and a solubility factor S

$$P = DS \tag{2}$$

Both D and S tend to depend on the local concentration of the permeating components in the feed and in the polymer, respectively, and can be evaluated by means of molecular modeling techniques.

For glassy polymers non-linear gas sorption has been described by the dual-mode sorption model that utilizes, in its simplest form, a two-term sorption isotherm. One term concerns Henry's law dissolution dependence of the concentration on the penetrant pressure while the other term is of a Langmuir type:

$$C = C_D + C_H = k_D p + C_H' bp/(1 + bp) \tag{3}$$

where C is the total concentration, C_D the concentration of a dissolved "population" into a low-molecular weight liquid or rubbery polymers (described by Henry's relation) and C_H the concentration of penetrants adsorbed in the so-called unrelaxed volume or in microvoids present in glassy polymers (described as a Langmuir "hole filling" process) [26]. k_D is the Henry's law constant, p the penetrant pressure, C_H' and b the Langmuir capacity constant and affinity constant, respectively.

Gas transport is attributed to diffusion of "dissolved" molecules while "adsorbed" molecules are assumed to be nearly immobilized.

A competing transport model of dual mode sorption expresses the local flux as being due to two contributions associated to two sorbed "populations" with different mobility and at local equilibrium with each other [27].

There are also other models for the diffusion of small molecules in glassy polymers, such as the free-volume diffusion model originally developed by Cohen and Turnbull [28] and then applied to polymers by Fujita [29]. This theory has been quite successful in explaining the diffusion of gas molecules in polymers [30,31]. No molecular information is however provided by this model.

Another theory is the molecular theory [32,33] and the Pace and Datyner model [34], in which a micromolecular transport mechanism is described via activated jumps. The authors postulated polymer bundles allowing two kinds of motion for the penetrant molecules: one parallel and the other across the chains. The jump through the bundle is possible when segments of appropriate size on two neighboring chains bend away from each other forming an opening through which the penetrant can pass. The movement along the chain is preferred requiring less activated energy. However, diffusion coefficients cannot be directly estimated because the movement is interrupted by entanglements that introduce jump lengths across the chains.

At the atomistic level, the real molecular composition and structure has to be considered in detail, and the diffusion of small gas molecules across the membrane has to be described considering the thermal vibrations of the polymer matrix on the transport. The results of MD-simulations showed two kinds of motion: movements in voids and jumps between neighboring free volume regions. In particular, it has been stated that over relatively long periods of time (about hundreds of picoseconds) the gas molecules explore distinct holes in the free volume in the polymer. From time to time, fluctuation channels open up and when they are wide enough the penetrants may jump through them. The related diffusion coefficients are completely determined by the jump events.

In this paper, a series of MD simulations with gas molecules (O_2, N_2 and H_2) in a glassy poly(ether–ether–ketone) membrane is reported.

The poly(ether–ether–ketone)s are well established as commercially important, high-performance engineering thermoplastics. During the last decade, considerable effort was made to produce modifications of the chemical nature of this class of polymers while maintaining their excellent physical properties to find membrane applications in electrodialysis, gas dehumidification and gas separation [35,36].

The incorporation of a phtalido group follows this trend producing an amorphous PEEK-WC (poly(oxa-*p*-phenylene-3,3-phtalido-*p*-phenylenoxoxa-*p*-phenylenexoxi-*p*-phenylene)) with a higher T_g (T_gPEEK-WC = 228°C; T_gPEEK = 143°C) and suitable for the preparation of membranes with inversion phase technique.

The investigations analyze the free volume distribution and the diffusive process in the bulk of this material. Furthermore, solubility and diffusion coefficients have been calculated utilizing the Gusev–Suter transition state method[3] [37–39].

Fluctuations of polymer matrix and the effect on the rate of jumps have been observed. In addition, sorptions of CH_4 of CO_2 have been calculated with the sorption module of MSI [40]. Results have been compared with experimental sorption isotherms of carbon dioxide showing a good agreement. To predict sorptive behavior quantitatively, methane was included in this study.

[3] The Gusev–Suter computations were performed using *gsnet* and *gsdif* programs developed by A. Tiller of Molecular Simulation Inc.

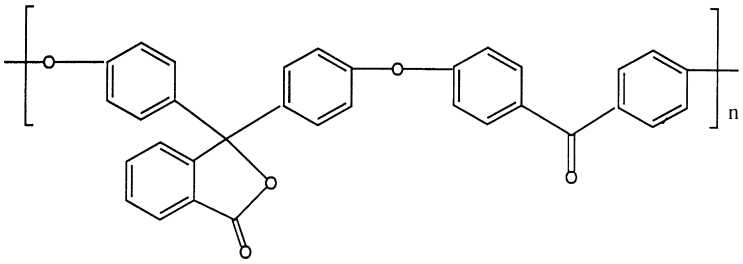

Fig. 1. Structure formulae of the repeat unit of PEEK-WC.

2. Packing models and simulation details

The structures investigated of poly(ether–ether–ketone)s were constructed and simulated by means of Insight/Discover software of Molecular Simulations Inc. [41] For the potential energy, the pcff forcefield was applied for all simulations. The calculation was performed on IBM RS 6000 and SGI ONYX workstations.

Two bulk models of PEEK-WC (PEEK-WC1 and PEEK-WC2) were built in several stages. The first step was the construction of the monomer (see Fig. 1). Then initial polymer structures were grown with the Polymerizer and Amorphous Cell modules [41] of the MSI software, which implement a modification of the rotational isomeric state (RIS) method of Theodorou and Suter [42,43]. The polymer chain was constructed at 303 K under cubic periodic boundary conditions; to have chain effects reduced, only one long chain, containing 51 monomer units (i.e. 3000 atoms), instead of several shorter chains segments was filled in each simulation box. This procedure was chosen to come closer to reality where polymer chains are typically composed of at least several thousand atoms. It is, however, to be mentioned that during the typical simulation times of a few nanoseconds used in the context of this paper, the molecular weight of the model chains should have only a very limited influence on the simulated small molecule separation properties.

Finally, considering the periodic boundary conditions, all atoms were inserted into the cell and the cell volume was consequently chosen to reproduce a final density of 1.25 g/cm^3. After all packing and equilibration stages eight oxygen, eight nitrogen and eight hydrogen gas molecules were inserted during this stage into separated locations of the unit cell.

The generation of an initial polymer structure is based on the "self-avoiding" random walk method of Theodorou and Suter [42]: this means that for building the initial polymer structure resembling the equilibrium structure as much as possible, the correct statistics for the dihedral angles of polymer chain conformations had to be reproduced.

The chain is constructed by first placing into the simulation box three subsequent backbone bonds with pendant atoms in some random orientation, and then growing one bond at time the polymer chain producing trial configurations with Boltzmann probabilities.

During this stage various possible choices of rotational

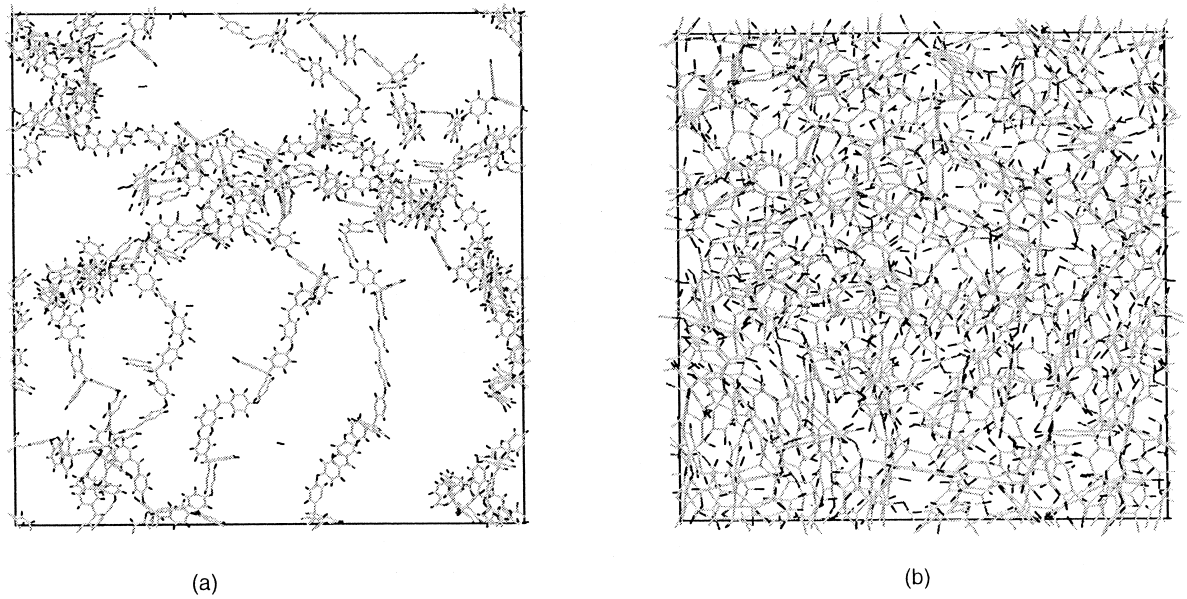

Fig. 2. (a) and (b) Initial and final (after refinement) amorphous polymer packing models: (a) PEEK-WC1 and (b) PEEK-WC2.

Table 1
Forcefield scaling for packing refinements

Number of stage	Scaling factor for conformational terms	Type of non bond terms	Scaling factor for *van der Waals* radii
For the first procedure			
1	0.001	quartic	0.5
2	0.1	quartic	0.5
3	0.1	quartic	1
4	1	quartic	1
5	1	6-12 Lennard-Jones	1
For the second procedure			
1	0.001	quartic	0.5
2	0.1	quartic	0.5
3	0.1	quartic	1.33
4	1	quartic	1.5
5	1	6-12 Lennard-Jones	1
6	1	6-12 Lennard-Jones	1

states for all relevant conformations of minimum energy are determined according to a set of probability functions using the standard Monte Carlo method.

Intermolecular overlaps between allowed rotational states are controlled by a modified probability associated with the variation of potential energy as additional criterion for the applied Metropolis calculations.

For the sake of efficiency of the packing algorithm, however, it was necessary to allow still some overlap between adjacent chain segments which later needs to be removed by equilibration procedures. In addition, to avoid packing algorithm related catenations and spearings of aromatic units, it was necessary to start the packing at a very low density of 0.1 g/cm^3 (cf. Fig. 2(a)).

Minimum image periodic boundary conditions, a cut-off distance for all non-bond interactions of 15 Å with a switching function of 1.5 Å were used for the subsequent equilibration and simulation stages. In the beginning, the initial packing models were subjected to sequences of static structure optimizations and NVT-MD runs combined with different procedures of forcefield scaling (cf. Table 1.

After this stage, the experimental density was reached by increasing the pressure with several cycles of NPT (constant particle number, temperature and pressure) runs at pressures of thousands of bars. Subsequently, simulated annealing with temperatures up to 1000 K was also necessary to equilibrate the compressed systems. The equilibrated packing model was then subjected to NVT-MD data production runs at a density of 1.23 g/cm^3.

These simulations were performed at 303 K for a total of 2.1 (model PEEK-WC1) and 3 ns (model PEEK-WC2), respectively. Newton's equation of motion was solved with a time step of 1 fs. The positions and velocities of all atoms of the model structures were saved each 500 ps in a history file.

Parallel to the MD simulations, the completely equilibrated packing models were subjected to the transition state theory algorithm developed by Gusev and Suter[3] [37–39]. The method permits estimation of diffusion and solubility constants of small gas molecules assuming that the polymeric matrix has to undergo only elastic fluctuations to accommodate the guest molecules.

In the Gusev–Suter method, a three-dimensional grid is layered over a completely equilibrated amorphous array. Then, inserting a gas probe molecule on each position of the grid, the interaction energy between the gas molecule and all host atoms was calculated utilizing a Lennard-Jones function.

Using these energy values, the whole packing cell was separated in regions of free volume with low energy and regions of densely packed polymer with high-interaction energy. Then, energetically favorable transition paths between adjacent holes, with a Boltzmann factor of jump probability assigned, were identified. Having determined appropriate jump probabilities, the diffusion of gas particles can be simulated via an MC type procedure. The main advantage of this method is that it needs much less computer simulation time than MD. There is, however a loss of atomistic detail as compared with MD.

The adsorption of diffusive gas molecules through the polymeric matrix was calculated by means of Sorption software of MSI [40]. These simulations were performed using a Grand Canonical Monte Carlo method. The sorption isotherm is computed considering an average number of guest sorbate molecules in equilibrium between the chemical potential of the sorbate gas and of a bulk gas at a defined temperature and pressure. The result is furnished as particle population density vs defined pressure $S = \langle N \rangle / P$. The interaction energy between particles and matrix are computed as averaged over the full production set of sampled configurations and is described by the short-range van der Waals interaction and the longer range electrostatic or Coulombic interaction.

In order to compare experimental and simulated permeability coefficients, we have calculated diffusion coefficients and solubilities of different gases. The coefficient of diffusion D has been calculated from the center-of-mass mean square displacement of the gas molecules $\mathrm{msd}(t) = \langle |\mathbf{R}(t) - \mathbf{R}(0)|^2 \rangle$ from the Gusev–Suter MC-simulation. The angle brackets refer to averages over all penetrant molecules and over all time origins.

Assuming that the diffusion has reached, the hydrodynamic limit D can be calculated from the Einstein relation

$$D = \langle |\mathbf{R}(t) - \mathbf{R}(0)|^2 \rangle / 6t \tag{4}$$

with $\mathbf{R}(t)$ being the Cartesian position vector describing the displacement of a permeant molecule from its origin. Eq. (3) could in principle also be used to determine D-values

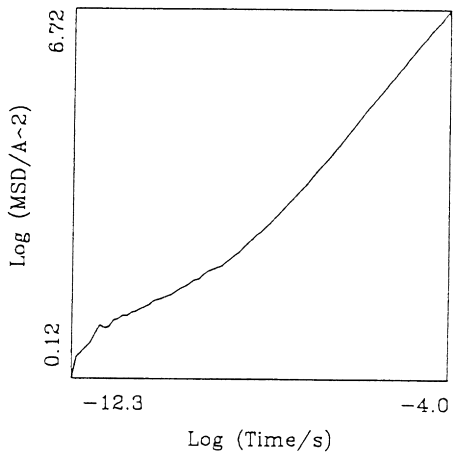

Fig. 3. Log[$s(t)$] vs. log(t) plot obtained for the diffusion of a hydrogen molecules in the model PEEK-WC2 from the Gusev–Suter procedure

directly from MD-simulations of the diffusive transport of small molecules. In evaluating the Einstein equations, one has, however, to consider possible effects of anomalous diffusion first reported by Müller-Plathe et al. [1]. The problem here is that Eq. (3) relies on the assumption of a random walk for each simulated particle through the polymer matrix. This means that the jumps of the gas molecules between individual holes in the free volume must determine the diffusive trajectory of the respective particle. The still rather short possible timescale of completely atomistic MD simulations (up to 10 ns) does, however, in the given and in many other cases, results in a non-negligible influence of the very fast movement of penetrant molecules (timescale several hundred picoseconds) inside the individual holes on the diffusion trajectories. This in-hole motion is determined by the shape of the holes and is therefore no random walk. Due to the mentioned effects, it was not possible in the given case to utilize the simulated MD trajectories directly for the determination of constants of diffusion.

The solubility S is also determined from the Gusev–Suter procedure. S gives the concentration c of a gas in a volume element of the polymer that is in equilibrium with an outside pressure reservoir of the same gas. The determination of S is done inserting gas particles in the refined polymer structure and then calculating the interaction energy. In the Gusev–Suter method, the insertion of gas particles into the simulation box is performed on all grid points of the cubic lattice layered onto the packing model.

Then the excess of thermodynamic potential μ_{ex} is calculated via

$$\mu\mathrm{ex} = \mathrm{R}T\ \ln\langle\exp(-E/\mathrm{k}T)\rangle \tag{5}$$

and S is then obtained from the following relation:

$$S = \exp(-\mu\mathrm{ex}/\mathrm{R}T) \tag{6}$$

with k and R being the Boltzmann and gas constant, respectively.

Table 2
Estimated and experimental permeability coefficients (units of permeability (Ba): Ba = [cm^3(SPT)cm/cm^2 s cmHg] 10^{-10})

Polymer	Gas	$P_{calc.}$ (Ba)	$P_{exp.}$ [a] (Ba)	$P_{exp.}$ [b] (Ba)
PEEK-WC	O_2	0.44	0.55	1[c]
	CO_2	3.37	2.71	3[c]
	N_2	0.04	< 0.1[d]	0.2[c]
	H_2	16.00	n.a.	6.0[c]
	He	112.00	6.99	3.0[c]
	CH_4	0.022	n.a.	0.08[c]

[a] Ref. [45].
[b] Ref. [46].
[c] In case of nitrogen the authors have not measured the permeability value because of the very low value (less than 0.1 Ba).
[d] All permeability data have been extrapolated from Arrhenius plot.

3. Results and discussion

The quality of the packing model had to be checked with the Gusev–Suter Monte Carlo method because it is not possible to run molecular dynamics simulations long enough to reach the normal diffusive regime and to get reasonable quantitative predictions of diffusivities in glassy polymers.

Fig. 3 shows the mean squared displacement plot of the Gusev–Suter runs. It follows a general trend observable in glassy polymers. Table 2 shows comparison between calculated and measured permeabilities for several gases in PEEK-WC. Except for Helium the deviations between the respective pairs of values are not considerably greater than a factor of about 3. Judging these results is to be noticed that the possible errors of experimental solubility and diffusivity data can be quite high. This is due to difficulties in obtaining really amorphous polymeric materials. It is, therefore, generally accepted that a coincidence between measured and simulated diffusivity and solubility values within a factor of 3–5 is still acceptable (cf. e.g. Ref. [2]). Therefore, in the given case, the investigated PEEK-WC packing models can be considered to be reasonably equilibrated at least as far as the correct representation of transport properties is concerned.

Table 2 lists values of permeability, P, at 303 K estimated from Transition State theory calculations for O_2, CO_2, N_2, H_2, He and CH_4 in the poly(ether–ether–ketone) membrane and lists also the comparison of the corresponding experimental values reported in literature [45,46]. The theoretical values are averaged for two simulation packing models, which did not differ significantly in their transport behavior.

The accuracy of calculated P-values depends on several factors: the forcefield used, the overall simulation time, the cut-off and other assumptions and approximations embodied in the MD simulations [13]. The experimental values of all gases refer to permeability data; no values are reported of D and S. The values of Golemme et al. [45] have been measured at 298 K. From the D and S data obtained from

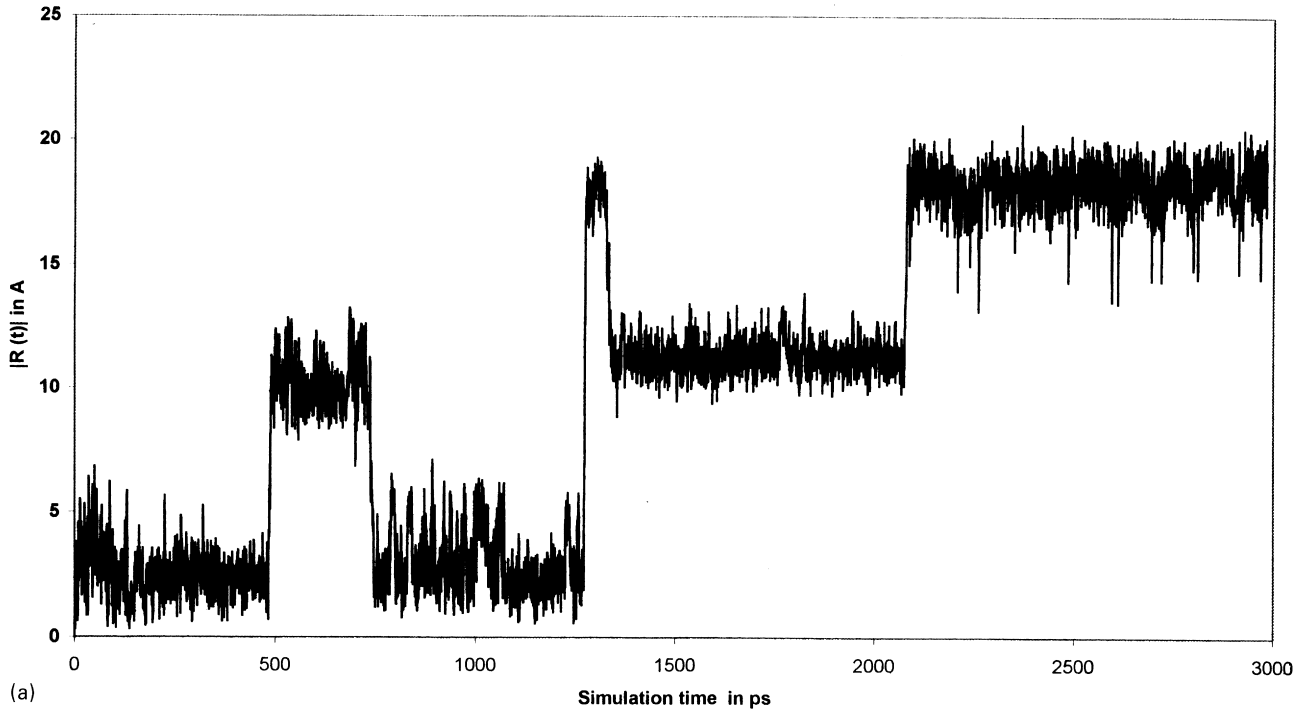

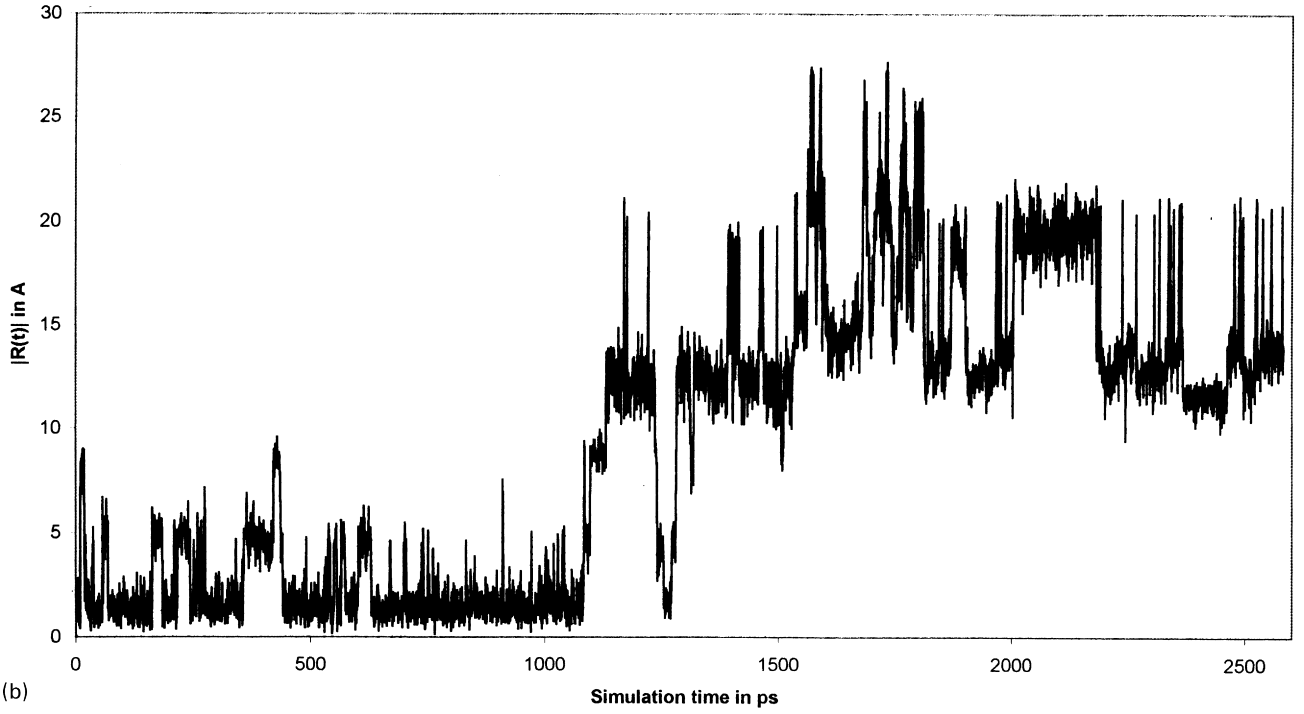

Fig. 4(a) and (b). Displacement $|R(t)| = \sqrt{|\mathbf{r}(t) - \mathbf{r}(0)|^2}$ of the oxygen (O7) and hydrogen (H5) molecule from their origins through the second simulation box (PEEK-WC2) as a function of the simulation time.

MD simulations, P was calculated via $P = DS$. The permeabilities of O_2 and CO_2, differ only by about 20–40% from the corresponding experimental ones which is a pretty good coincidence. Also, still acceptable are the results for H_2, N_2 and CH_4. Only the simulated He data are much higher than the experimental values. This latter finding may be attributable to a non-jump diffusion mechanism for this gas, which would be contradictory to the assumptions made in the Gusev–Suter method.

Thus, in general the agreement between calculated and experimental data can be considered reasonable indicating that the packing models are of acceptable quality and that

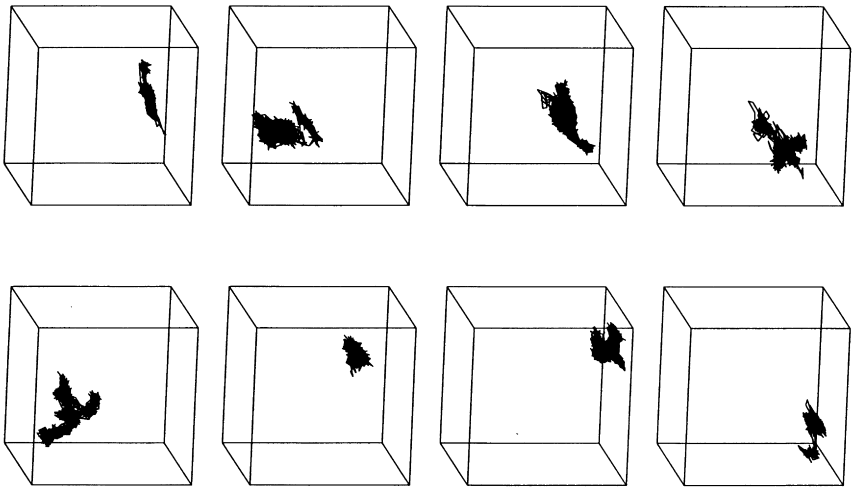

Fig. 5. Nitrogen trajectories in the model PEEK-WC2. The size of the cubes corresponds to the volume of the simulated basic volume element.

basic features of the gas diffusion process can be correctly described.

The simplest way of studying diffusion of individual penetrants is to inspect their paths through space. A procedure often chosen in the literature is to analyze the mean squared displacement msd(t) averaged over all penetrant molecules of a given kind. In order to get a more detailed insight in different modes of penetrant molecules, it can also make sense to investigate displacement $|R(t)|$ and msd(t) for individual penetrants [19].

Over the simulation time, some particles may just remain in one and the same hole, may jump back and forth between one and the same two adjacent holes or may perform jumps between a larger number of holes. Fig. 4(a) and (b) show the displacement $|R(t)| = \sqrt{|\mathbf{r}(t) - \mathbf{r}(0)|^2}$ of an oxygen and an hydrogen molecule, respectively, from its initial position $\mathbf{r}(0)$ in one of the two simulation boxes. This graph illustrates a common motion pattern for a molecule moving in an amorphous polymer. It can be recognized that particles move oscillating in a spatial range of few angstroms, which means in the same void for hundreds of picoseconds. The amplitude of the oscillations depends on the size of the visited hole. These positional fluctuations are not effective for the diffusive behavior. From time to time this mode of motion is followed by a jump into an adjacent hole. These jumps take only a few picoseconds to occur.

Figs. 5–7 contain the trajectories of the three gases (hydrogen, nitrogen and oxygen) in the simulated box. These figures, revealing the path of each gas molecule through the matrix, indicate the shape of visited free volumes. It can be recognized that each gas molecule moves in rather small spatial regions before jumping to an adjacent hole. The faster movement of hydrogen as compared with oxygen and nitrogen is visible by the larger size of the visited volume.

Besides the predictive capabilities concerning quantitative transport parameters, MD simulations are a powerful tool to furnish deeper insights in the structure and the

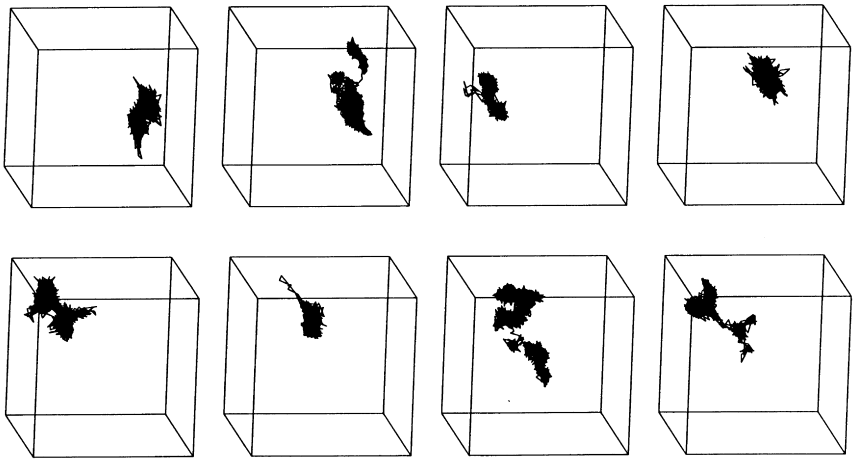

Fig. 6. Oxygen trajectories in the model PEEK-WC2. The size of the cubes corresponds to the volume of the simulated basic volume element.

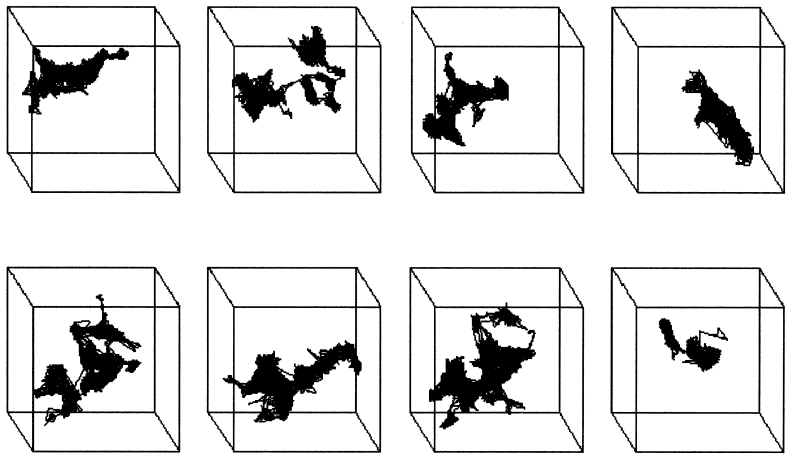

Fig. 7. Hydrogen trajectories in the model PEEK-WC2. The size of the cubes corresponds to the volume of the simulated basic volume element.

dynamic behavior of simulated polymers. Thus, the distribution of free volume, the mobility of the polymeric chains and details of the movements of each gas molecules through the matrix can be directly checked.

Fig. 8 contains a series of 0.35 nm thick slices cut through the equilibrated PEEK-WC2 packing model. Pictures of this kind showing the whole packing cell as a series of slices at a specific simulation time can give an idea about the molecular packing status (including the free volume distribution) of dense stiff chain glassy polymers. The comparison with some polyimides simulated in a similar way (cf. Refs. [19,44,47]) shows that the investigated PEEK-WC has a relatively small amount of free volume. Particularly, the size of accessible individual holes is considerably lower for PEEK-WC than for the mentioned polyimides as can be seen from Fig. 9. Not surprisingly, the polyimide shown in this figure revealed much higher diffusivity- and solubility-values for gas molecules (e.g. $D_{O2} = 7 * 10^{-7}$ cm^2/s, $S_{o2} = 2.2 * \text{bar}^{-1}$) than PEEK-WC (cf. Table 2).

Fig. 10 shows the movement of an oxygen molecule through the polymer matrix in PEEK-WC1 during a jump event. For this purpose, one suited slice of a thickness of 3.5 Å was cut perpendicular to the *x*-axis through the model. In Fig. 10, this slice is displayed at different simulation times between $t = 385$ and 389 ps. It is possible to observe that in cooperation with the displacement of the gas molecule along the polymer, temporary fluctuations of the matrix connected with the formation of a channel between two

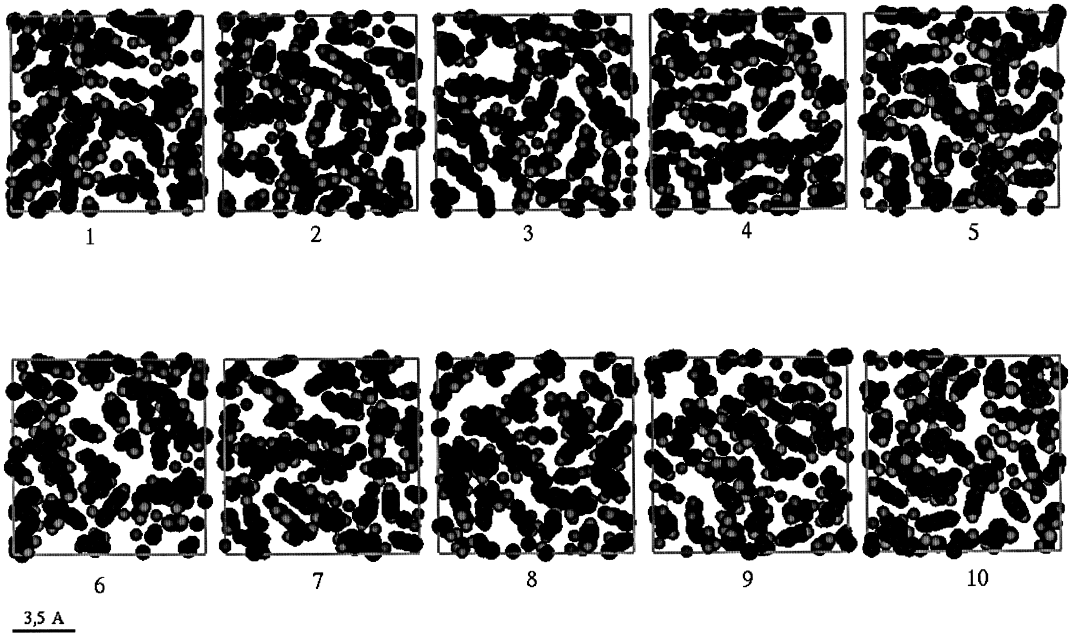

Fig. 8. Series of 0.35 nm thick slices cut along the *z*-axis of a well equilibrated PEEK-WC2 model of density 1.24 g cm^{-3}. **1** is the top slice, **10** is the bottom slice.

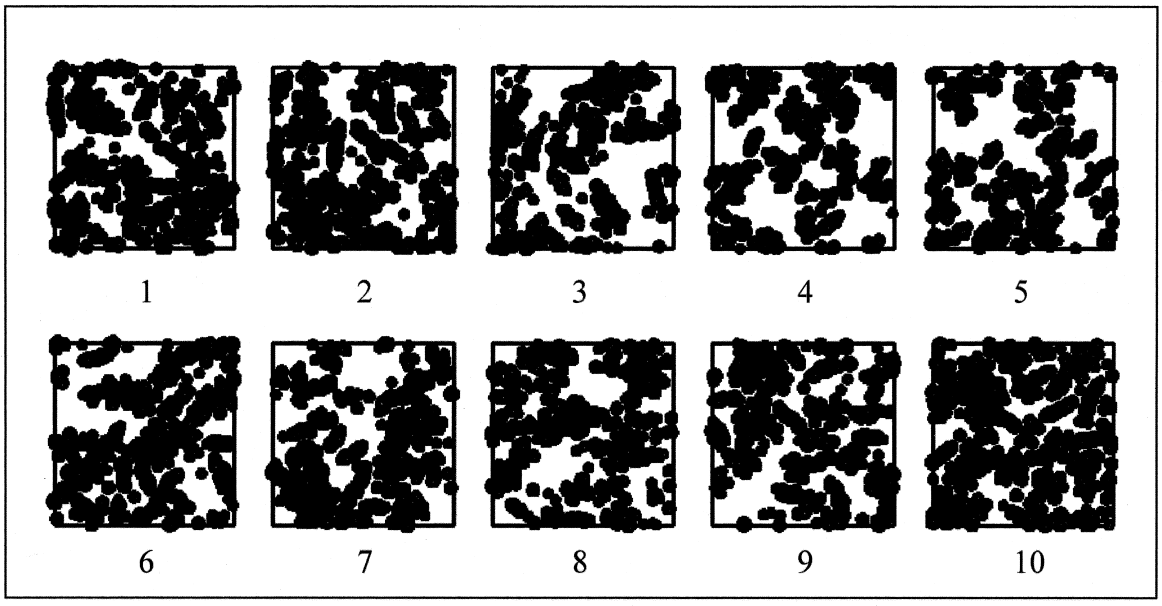

PI1

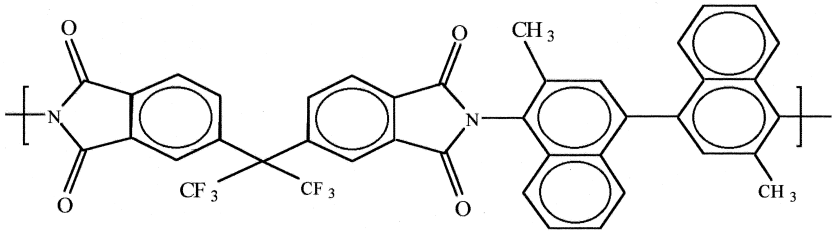

Fig. 9. Series of 0.33 nm thick slices cut along the *z*-axis of a well equilibrated model of the polyimide PI1 shown at the bottom. **1** is the top slice, **10** is the bottom slice.

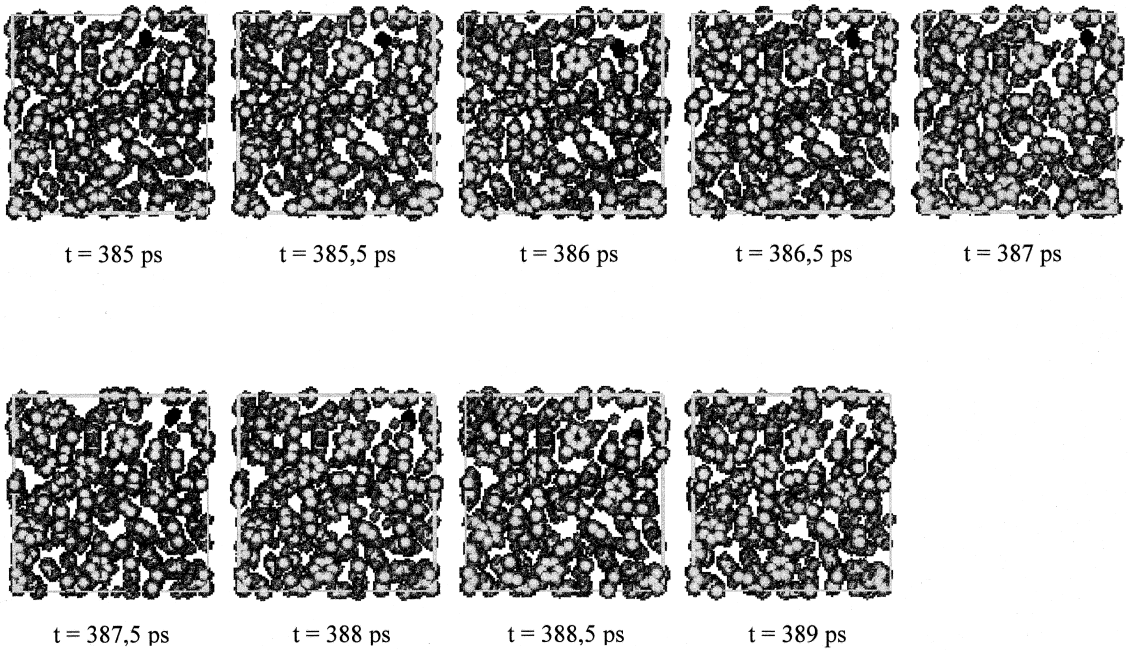

Fig. 10. Series of slices 3.5 Å thick cut along the *x*-axis showing a jump even to an oxygen molecule occurred between $t = 385$ and 389 ps in the PEEK-WC1 model. The black color in the picture is the oxygen molecule, the grey for the polymer atoms.

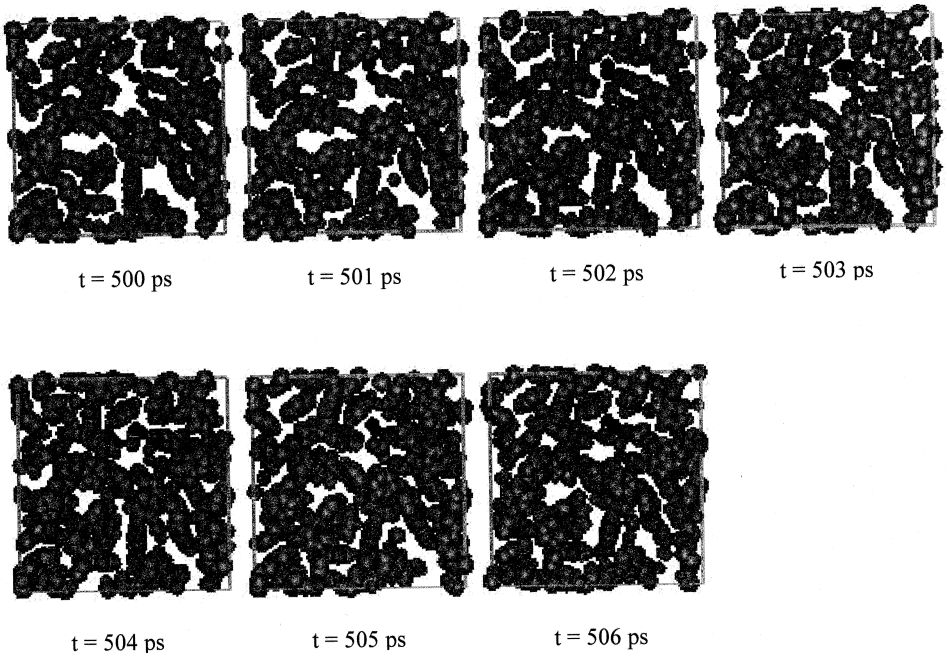

Fig. 11. Series of slices 3.5 Å thick cut along the *x*-axis showing a jump of an hydrogen molecule occurred between $t = 500$ and 530 ps in the PEEK-WC2 model. The black color in the picture is the oxygen molecule, the grey for the polymer atoms.

adjacent holes are evident. These thermal fluctuations are, however, less remarkable than for flexible polymer chains [12,29].

A similar behavior is observable in Fig. 11 showing another jump event for a hydrogen molecule occurring between $t = 500$ and 506 ps with the help of a slice of 0.35 nm thickness cut perpendicular to the *y*-axis of the PEEK-WC2 model. Both pictures confirm the usual small-molecule diffusion mechanism via jumps through temporary channels. Over the short intervals of simulation time of 4 and 30 ps shown in Figs. 10 and 11, respectively, the observable overall segmental motion of the polymer are as expected smaller than for rubbery flexible chain polymers like PDMS (cf. Ref. [12]) or POMS (cf. Ref. [44]). The reduced mobility of the PEEK-WC structure is essentially due to the presence of the ether–ether rings and the other large aromatic segments.

In rubbery flexible chain polymers like PDMS, atomistic

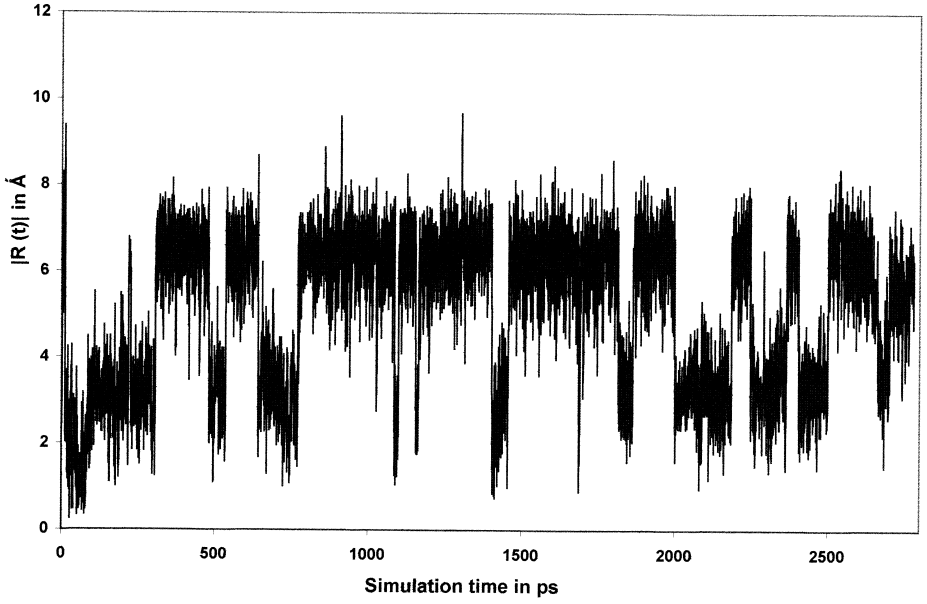

Fig. 12. Displacement $|\mathbf{R(t)}|$ of a penetrating hydrogen molecule from its origin in the PEEK-WC2 model as function of the simulation time **t**. The diffusion process is characterized by a typical rate that jumps back and forth between two adjacent voids in the polymer matrix.

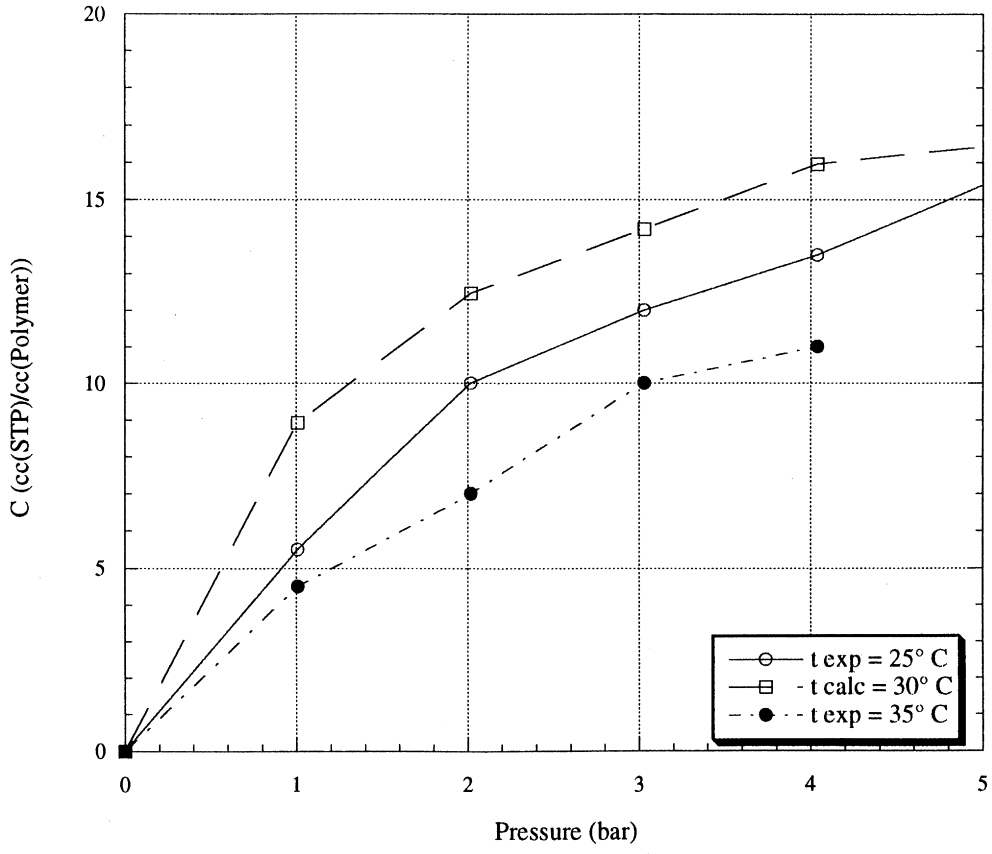

Fig. 13. Simulated sorption isotherms of CO_2 at 300 K in comparison with experimental data [45].

transport simulations (cf. e.g. Refs. [44,47]) indicated that the lifetime of temporary channels is within a range of a few picoseconds and thus much lower than the average residence time of a penetrant molecule in one and the same hole which is about 100 ps or more. This leads to a diffusion mechanism, which already over times of a few hundred picoseconds results in a relatively straightforward displacement of penetrant molecules from their origin.

As for the already mentioned polyimides (cf. Refs. [19,44,47]), also for poly(ether–ether–ketone, PEEK-WC, a high percentage of penetrant molecules just jumping back and forth between two neighboring holes for times up to several nanoseconds was observed. This finding was related with the lifetime of temporary channels between different parts of the free volume. In difference to the flexible chain rubbery polymer case, this lifetime is much longer than the average residence time of a diffusing molecule in a cavity. As long as such a channel is open, it is energetically much more favorable for a penetrant molecule to use this channel again and again to keep jumping between two particular holes instead of moving to a third one that is separated by a higher energy barrier. For the understanding of small molecule diffusion in stiff chain glassy polymers, it is important to recognize, that each pair of jumps of a penetrant molecule back and forth between one and the same two holes does basically not contribute to its diffusion through the polymer. This kind of behavior is certainly a major reason for the general tendency that constants of diffusion for small molecules in dense amorphous polymers are smaller for the glassy stiff chain case than for the rubbery flexible chain case if similar relative amounts of free volume can be assumed.

In the case of PEEK-WC, there is a relatively small fraction of free volume (Fig. 8) and the redistribution of polymer segments is so slow that as in the case of the polyimides, channels between adjacent cavities have relatively long lifetime. Therefore, also the effect of back jumps of penetrant gases has been observed for the three gases inserted into the polymer matrix (O_2, N_2 and H_2). Fig. 12 displays this situation, where in this case an hydrogen molecule in the PEEK-WC2 model over the whole simulation time keeps jumping back and forth between one and the same two voids of the polymer matrix.

Fig. 13 contains the sorption isotherm of CO_2 calculated at 300 K. The shape is typical of glassy polymers. The simulation technique can describe completely the sorption behavior (both Henry and non-Henry). The comparison with experimental isotherm measured at 25, 35 and 45°C [45] reveals that dissolution in simulation is increased in comparison with experimental data. Because the narrow range of

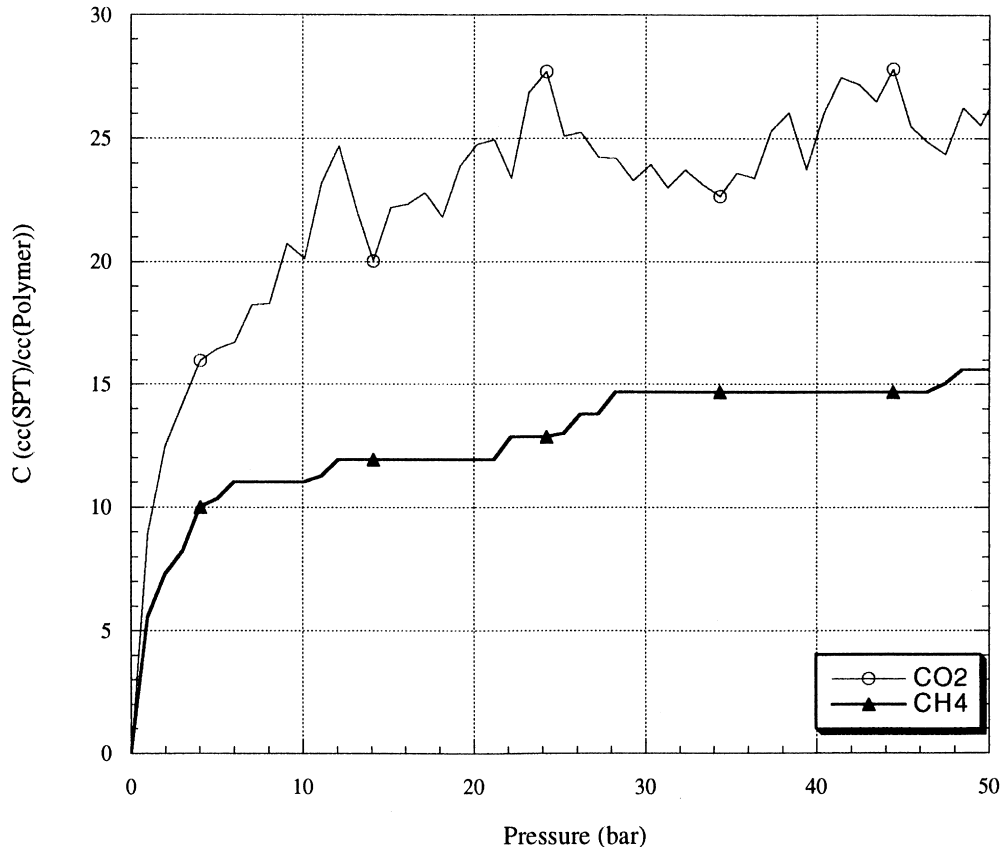

Fig. 14. Simulated sorption isotherms of CH_4 and CO_2.

the pressure employed in the calculation of experimental data, it is not possible to compare the full curve.

In general, the agreement between calculated and experimental data can be considered acceptable assuming errors in GCMC technique and the errors in the experimental data. In addition, sorptions of CH_4 has been calculated to predict sorptive behavior quantitatively of methane (see Fig. 14).

4. Conclusions

This paper examines the diffusion behavior of oxygen, nitrogen and hydrogen molecules through a cardo poly(-ether–ether–ketone glassy amorphous polymer model of size of about 30 Å. Atomistic MD simulations of about 3 ns were undertaken and the Gusev–Suter Transition State MC method has been used to calculate permeabilities, extending diffusion simulation beyond the anomalous region. With this technique, acceptable agreement between calculated and measured data has been reached.

Also sorption isotherm of carbon dioxide was simulated via GCMC method showing a considerable coincidence with the experimental ones. To predict sorptive behavior quantitatively, methane was also included in this study. Atomistic details about the mechanism of transport process were evaluated. Qualitatively the diffusion of each gas molecule proceeds by hopping mechanism, i.e. small penetrants oscillate for longer period of time around certain positions and perform quick jumps in a neighboring region. Static free volume distribution into the bulk model was visualized.

The differences found, also in Hofmann et al. [44], about the diffusion of penetrants through stiff glassy and flexible rubbery polymers can be confirmed also in the case of cardo poly(ether–ether–ketone)s, PEEK-WC. The increased rigidity of chain in comparison with the glassy polyimides produces important effects such as back jumps of penetrant molecules from a “just reached hole to hole” (also visible from the displacement of $|\mathbf{R}(t)|$ of individual molecule). We have found that PEEK-WC has a more rigid structure: channels between adjacent parts of the free volume are open longer than polyimides flexible PDMS [44]. This can be a confirmation of what found in literature for the lower permeabilities in stiff chain polymers.

References

[1] Gusev AA, Muller-Plathe F, van Gunsteren WF, Suter UW. Adv Polym Sci 1994;16:207–47.
[2] Muller-Plathe F. Acta Polym 1994;45:259.
[3] Shah VM, Stern SA, Ludovice PJ. Macromolecules 1989;22: 4660–2.

[4] Sok RM, Berendsen HJB. Polym Prepr 1992;33:641–2.
[5] Trohalaki S, Rigby D, Kloczkowski A, Mark JE, Roe RJ. In: Roe RJ, editor. Computer simulation of polymers, Englewood Cliffs, NJ: Prentice-Hall, 1991. p. 220–32.
[6] Takeuchi H, Okazaki K. J Chem Phys 1990;92:5643–52.
[7] Sonnenburg J, Gao J, Weiner JH. Macromolecules 1990;23: 4653–7.
[8] Boyd RH, Krishna Pant PV. Macromolecules 1991;24:6325–31.
[9] Krishna Pant PV, Boyd RH. Macromolecules 1993;26:679–86.
[10] Sok RM, Berendsen HJB, van Gunsteren WF. J Chem Phys 1992;96:4699–704.
[11] Muller-Plathe F, Rogers SC, van Gunsteren WF. Chem Phys Lett 1992;199:237–43.
[12] Fritz L, Hofmann D. Polymer 1997;38:1035–45.
[13] Fritz L, Hofmann D. Polymer 1998;39:2531–6.
[14] Charati SG, Stern SA. Macromolecules 1998;31:5529–35.
[15] Takeuchi H. J Chem Phys 1990;93:2062–7.
[16] Muller-Plathe F. J Chem Phys 1991;94:3192–9.
[17] Krishna Pant PV, Boyd RH. Macromolecules 1992;25:494–5.
[18] Smith E, Mulder MHV, Smolder CA, Karrenbeld H, van Eerden J, Feil D. J Membr Sci 1992;73:247–57.
[19] Hofmann D, Ulbrich J, Fritsch D, Paul D. Polymer 1996;27: 4773–85.
[20] Zhang R, Mattice WL. J Membr Sci 1995;108:15–23.
[21] Chen CL, Lee CL, Chen HL, Shih JH. Macromolecules 1994;27:7872.
[22] Puri PS. International Conference on Membrane Science and Technology (ICMST'98), China, 1998.
[23] Stern SA. J Membr Sci 1994;94:1–65.
[24] Wijmans JG, Baker RW. J Membr Sci 1995;107:1–21.
[25] Crank J. The mathematics of diffusion. 2nd ed. Oxford: Clarendon Press, 1975.
[26] Koros WJ, Chern RT. In: Rousseau RW, editor. Handbook of separation process technology, New York: Wiley, 1987. p. 862–953.
[27] Paul DR, Koros WJ. J Polym Sci, Polym Phys Ed 1978;14:675.
[28] Cohen MH, Turnbull D. J Chem Phys 1959;31:1164.
[29] Fujita H. Fortschr Hochpolym Forsch 1961;3:1.
[30] Ventras JS, Duda JL. J Appl Polym Sci 1978;24:2325.
[31] Stern SA, Sampat SR, Kulkarni SS. J Polym Sci 1986;24:2149.
[32] Brandt WW. J Chem Phys 1959;63:1080.
[33] Dibenedetto A. J Polym Sci 1963;1:3459 (see also p. 3477).
[34] Pace RJ, Datyner A. J Polym Sci, Polym Phys Ed 1979;17:473 (see also p. 453 and 465).
[35] Handa YP, Roovers J, Moulinie P. J Polym Sci: Part B: Polym Phys 1997;35:2355–62.
[36] Wang ZY, Moulinie PR, Handa YP. J Polym Sci: Part B: Polym Phys 1998;36:425–31.
[37] Gusev AA, Arizzi S, Suter UW. J Chem Phys 1993;99:2221.
[38] Gusev AA, Suter UW. J Chem Phys 1993;99:2228.
[39] Gusev AA, Suter UW. J Computer-aided Mater Design 1993;1:63.
[40] Catalysis User Guide, Sorption Section, Version 4.0.0 San Diego: MSI, 1996.
[41] Polymer User Guide, Amorphous Cell Section, Version 4.0.0 San Diego: MSI, 1996.
[42] Theodorou DN, Suter UW. Macromolecules 1985;18:1467.
[43] Theodorou DN, Suter UW. Macromolecules 1986;19:139.
[44] Hofmann D, Fritz L, Ulbrich J, Paul D. Polymer 1997;38(25):6145.
[45] Golemme G, Drioli E, Lufrano F. Polym Sci 1994;36(1):1647.
[46] Liu W, Chen T, Xu J. J Membr Sci 1990;53:203.
[47] Hofmann D, Fritz L, Ulbrich J, Paul D. Submitted for publication.